

Control of Stereoselectivity in the Ring-Opening Metathesis Polymerization of Norbornene by the Auxiliary Ligands Butadiene and *o*-Xylylene in Well-Defined Pentamethylcyclopentadiene Tantalum Carbene Complexes

Kazushi Mashima*

Department of Chemistry, Graduate School of Engineering Science, Osaka University,
Toyonaka, Osaka 560, Japan

Michitaka Kaidzu, Yoshiyuki Tanaka, Yuushou Nakayama, and
Akira Nakamura

Department of Macromolecular Science, Graduate School of Science, Osaka University,
Toyonaka, Osaka 560, Japan

James G. Hamilton and John J. Rooney

School of Chemistry, The Queen's University of Belfast, David Keir Building,
Belfast BT9 5AG, Northern Ireland

Received April 17, 1998

cis-Dialkyl complexes of tantalum, Ta(CH₂Ph)₂Cp*(η^4 -C₄H₆) (**2a**) (Cp* = η^5 -C₅Me₅), TaMe(CH₂SiMe₃)Cp*(η^4 -butadiene) (**6**), and TaMe(CH₂CMe₃)Cp*(η^4 -butadiene) (**7**), were found to be catalyst precursors for ring-opening metathesis polymerization (ROMP) of norbornene to give poly(norbornene) with a high *cis*-vinylene double-bond (97–99%) content, while an *o*-xylylene complex Ta(CH₂Ph)₂(η^4 -*o*-(CH₂)₂C₆H₄)Cp* (**9**) was also an initiator to give poly(norbornene) with a high *trans*-vinylene double-bond (92–95%) content. When a Cp–butadiene complex Ta(CH₂Ph)₂Cp(η^4 -C₄H₆) (**2b**) was used as an initiator, we obtained poly(norbornene) with no selectivity (1:1 mixture of *trans*- and *cis*-vinylene bonds). The factors controlling these stereoselectivities have been investigated, and we obtained the following results: (1) We isolated benzylidene complexes and found that the proportion of *anti*- and *syn*-rotamers obtained depended on the kind of auxiliary ligands on the tantalum center, i.e., 1,3-butadiene or *o*-xylylene. Thermolysis of **2a** in the presence of PMe₃ resulted in the formation of a benzylidene complex Ta(=CHPh)Cp*(η^4 -C₄H₆)(PMe₃) (**3a**) as an *anti*-rotamer, which has been characterized by X-ray crystal structure analysis, while a similar treatment of **2b** afforded Ta(=CHPh)Cp(η^4 -C₄H₆)(PMe₃) (**3b**), also in the *anti*-rotamer form, as revealed by a comparison of the chemical shift value of the benzylic proton of **3b** with that of **3a**. In sharp contrast to the *anti*-geometry, a benzylidene complex Ta(=CHPh)(η^4 -*o*-(CH₂)₂C₆H₄)Cp* (**12**), bearing an *o*-xylylene ligand instead of the butadiene ligand, was obtained by thermolysis of **9**. The X-ray crystal structure analysis of **12** revealed that it is a *syn*-rotamer and has three-legged piano stool geometry. (2) Metallacyclobutanes are considered as intermediates during the propagation step. We could not isolate any metallacyclobutane during the ROMP of norbornene; however, a tantalacyclobutane Cp*(η^4 -*o*-xylylene)Ta[CH(Ph)CH(C₁₀H₆)CH] (**15**) was isolated in 18% yield when acenaphthylene, instead of the norbornene, was added to **12**. The *trans*-phenyl geometry of the metallacyclobutane ring system, which indicated the retention of the Ta=C bond stereochemistry, was determined by the X-ray analysis of **15**, whose structural features were compared with that of Cp*(η^4 -butadiene)Nb[CH₂CH(C₁₀H₆)CH] (**14**). (3) In contrast to high *cis/trans* stereoselectivity, the stereoregularity or tacticity of the cyclopentane ring sequences in poly(norbornene) obtained by the tantalum complexes estimated from the ¹³C NMR spectra of the hydrogenated derivatives was found to be almost *atactic*. This suggests that the alkylidene species would be a resting state during the propagation, and thereby monomer could be added to both faces of the Ta=C bond, leading to the *atactic* polymer. Consequently, the high *cis* and *trans* stereoselectivity thus demonstrated is ascribed to the huge congestion between the Cp* ligand and auxiliary ligands 1,3-butadiene or *o*-xylylene.

Introduction

Alkylidene complexes of transition metals have attracted much interest since they have been used as catalysts as well as reagents for reactions such as alkene formation from carbonyl compounds, olefin metathesis, and ring-opening metathesis polymerization (ROMP) of cyclic olefins.^{1–6} Well-defined metathesis catalysts such as titanacyclobutanes,^{5,7–9} Mo(NR)(CHR')(OR'')₂,^{10–18} and RuCl₂(CHR)(PR')₃^{19–24} have recently proven useful in ROMP, have led to a more precise description of the whole mechanism, and have also achieved living ROMP with high selectivity. Generally, the properties of polymers sensitively depend not only on molecular weight and polydispersity but also on the microstructure of the polymer backbone. Poly(norbornene) and its derivatives are interesting materials as the control of polymer microstructure in terms of both the *cis/trans* double-bond ratio and the relative orientation of the cyclopentylene rings, i.e., tacticity, Figure 1, has provided a challenge.²⁵ Although recently a number of stereocontrolled polymerizations of norbornadiene derivatives have been reported,^{10–18} there are relatively few examples of the stereospecific polymerization of norbornene derivatives, and these have involved the use of classical catalyst systems such as ReCl₅²⁵ and OsCl₃,²⁶ which yield *cis syndiotactic* polymer and (mesitylene)-W(CO)₃,²⁵ which gave *trans isotactic* material.

Grubbs work on a titanocene–carbene system prompted us to study a new catalyst system based on the

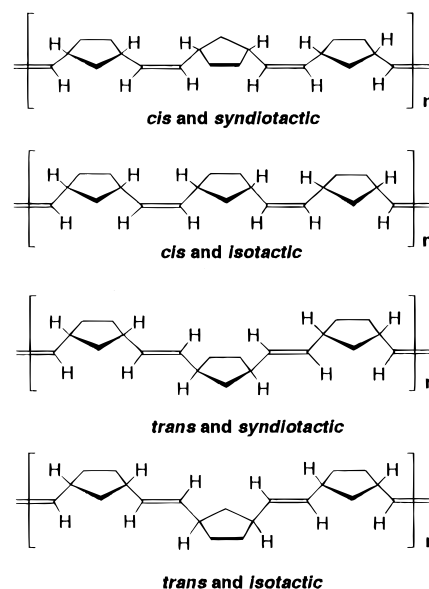


Figure 1. Four possible stereoregularities of poly(norbornene).

metallocene-like TaCp*(diene) (Cp* = pentamethylcyclopentadienyl) fragment, isoelectronic and isolobal to group 4 metallocene fragments Cp₂M, which are 14-electron species; we had found that TaCp*(diene) stabilized various reactive species such as benzyne²⁷ and cationic alkyls²⁸ similar to the corresponding metallocene complexes of group 4 metals. We prepared and characterized *cis*-dialkyl complexes bearing TaCp*(η^4 -butadiene), TaCp*(η^4 -butadiene), and TaCp*(η^4 -*o*-xylylene) fragments, and all these complexes were catalyst precursors for the ROMP of norbornene. We have found that a combination of Cp* and butadiene ligands affords a polymer having *cis*-vinylene bonds, while a combination of Cp* and *o*-xylylene ligands results in a *trans*-polymer; however, the Cp–butadiene system has no stereoselectivity. We have also found that these poly(norbornene)s were almost *atactic* on the basis of the ¹³C NMR spectra of the hydrogenated derivatives. The outline of a mechanism is discussed on the basis of the isolation of two kinds of benzyldiene complexes, an *anti*-rotamer for a butadiene complex and a *syn*-rotamer for an *o*-xylylene complex, together with metallacyclobutanes. A part of this work has been the subject of preliminary communications.²⁹

Results and Discussion

Synthesis of Catalyst Precursors and Benzyldiene Complexes. From Diene Complexes. A new series of *cis*-dialkyl complexes bearing 14-electron “Ta(η^5 -C₅R₅)(η^4 -C₄H₆)” (R = H, Me) fragments, which are isoelectronic to metallocene fragments of group 4 metals, were found to be catalyst precursors for the ROMP of norbornene. We have already communicated the synthesis and the crystal structure of the dibenzyl tantalum complex Ta(CH₂Ph)₂Cp*(η^4 -C₄H₆) (**2a**), which

(1) Nugent, W. A.; Meyer, J. M. *Metal–Ligand Multiple Bonds*; Wiley-Interscience: New York, 1988; p 133.

(2) For comprehensive reviews: Ivin, K. J. *Olefin Metathesis*; Academic Press: New York, 1983. Dragutan, V.; Balaban, A. T.; Dimonie, M. *Olefin Metathesis and Ring Opening Polymerization of Cyclo-Olefins*, 2nd ed.; Wiley-Interscience: New York, 1985. Ivin, K. J.; Mol, J. C. *Olefin Metathesis and Metathesis Polymerization*; Academic Press: London, 1997.

(3) Feldman, J.; Schrock, R. R. *Prog. Inorg. Chem.* **1991**, 39, 1.

(4) Schrock, R. R. *Acc. Chem. Res.* **1979**, 12, 98.

(5) Grubbs, R. H.; Tumas, W. *Science* **1989**, 243, 907.

(6) Novak, B. M.; Risse, W.; Grubbs, R. H. *Adv. Polym. Sci.* **1990**, 102, 47.

(7) Gilliom, L. R.; Grubbs, R. H. *J. Am. Chem. Soc.* **1986**, 108, 733.

(8) Petasis, N. A.; Fu, D.-K. *J. Am. Chem. Soc.* **1993**, 115, 7208.

(9) Grubbs, R. H.; Gilliom, L. R. *J. Mol. Catal.* **1988**, 46, 255.

(10) Bazan, G. C.; Khosravi, E.; Schrock, R. R.; Feast, W. J.; Gibson, V. C.; O'Regan, M. B.; Thomas, J. K.; Davis, W. M. *J. Am. Chem. Soc.* **1990**, 112, 8378.

(11) McConville, D. H.; Hofmeister, G. E.; Schrock, R. R. *J. Am. Chem. Soc.* **1993**, 115, 4413.

(12) Oskam, J. H.; Schrock, R. R. *J. Am. Chem. Soc.* **1993**, 115, 11831, and references therein.

(13) O'Dell, R.; McConville, D. H.; Hofmeister, G. E.; Schrock, R. R. *J. Am. Chem. Soc.* **1994**, 116, 3414, and references therein.

(14) Schrock, R. R.; Lee, J.-K.; O'Dell, R.; Oskam, J. H. *Macromolecules* **1995**, 28, 5933.

(15) Totland, K. M.; Boyd, T. J.; Lavoie, G. G.; Davis, W. M.; Schrock, R. R. *Macromolecules* **1996**, 29, 6114.

(16) Feast, W. J.; Gibson, V. C.; Marshall, E. L. *J. Chem. Soc., Chem. Commun.* **1992**, 1157.

(17) Feast, W. J.; Gibson, V. C.; Ivin, K. J.; Kenwright, A. M.; Khosravi, E. *J. Chem. Soc., Chem. Commun.* **1994**, 1399.

(18) Schrock, R. R. *Acc. Chem. Res.* **1990**, 23, 158.

(19) Nguyen, S. T.; Johnson, L. K.; Grubbs, R. H.; Ziller, J. W. *J. Am. Chem. Soc.* **1992**, 114, 3974.

(20) Nguyen, S. T.; Grubbs, R. H. *J. Am. Chem. Soc.* **1993**, 115, 9858.

(21) Lynn, D. M.; Kanaoka, S.; Grubbs, R. H. *J. Am. Chem. Soc.* **1996**, 118, 784, and references therein.

(22) Schwab, P.; Grubbs, R. H.; Ziller, J. W. *J. Am. Chem. Soc.* **1996**, 118, 100.

(23) Wilhelm, T. E.; Belderrain, T. R.; Brown, S. N.; Grubbs, R. H. *Organometallics* **1997**, 16, 3867.

(24) Belderrain, T. R.; Grubbs, R. H. *Organometallics* **1997**, 16, 4001.

(25) Hamilton, J. G. *Polymer*, in press.

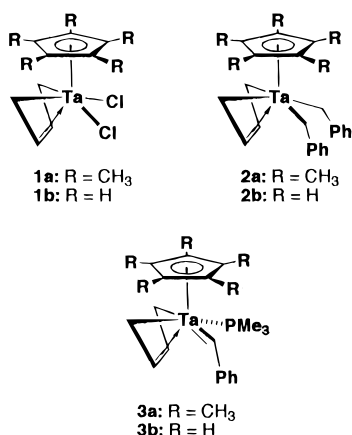
(26) Al-Samak, B.; Amir-Ebrahimi, V.; Carvill, A. G.; Hamilton, J. G.; Rooney, J. J. *Polymer Int.* **1996**, 41, 85.

(27) Mashima, K.; Tanaka, Y.; Nakamura, A. *Organometallics* **1995**, 14, 5642.

(28) Mashima, K.; Fujikawa, S.; Tanaka, Y.; Urata, H.; Oshiki, T.; Tanaka, E.; Nakamura, A. *Organometallics* **1995**, 14, 2633.

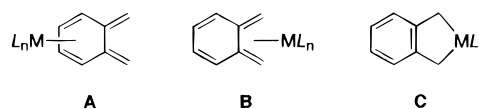
(29) Mashima, K.; Tanaka, Y.; Kaidzu, M.; Nakamura, A. *Organometallics* **1996**, 15, 2431.

was prepared in 83% yield by reaction of $\text{TaCl}_2\text{Cp}^*(\eta^4\text{-C}_4\text{H}_6)$ (**1a**) with 2 equiv of benzyl Grignard reagent in THF.²⁹ The Cp analogue $\text{Ta}(\text{CH}_2\text{Ph})_2\text{Cp}(\eta^4\text{-C}_4\text{H}_6)$ (**2b**) was obtained as brown crystals in 51% yield by a similar reaction of $\text{TaCl}_2\text{Cp}(\eta^4\text{-C}_4\text{H}_6)$ (**1b**) with 2 equiv of benzyl Grignard reagent in THF followed by recrystallization from a mixture of toluene and hexane. The structure of **2b** was characterized on the basis of NMR spectroscopy and compared with that found for **2a**. The ^1H NMR spectrum of **2b** showed AB type benzylic signals at δ 1.27 and 1.86 ($J = 10.9$ Hz) which are shifted to lower field compared to those (δ 0.40 and 1.23, $J = 10.9$ Hz) found for **2a**. We have already reported the thermolysis of **2a** in the presence of PMe_3 to afford a benzylidene complex $\text{Ta}(\text{=CHPh})\text{Cp}^*(\eta^4\text{-C}_4\text{H}_6)(\text{PMe}_3)$ (**3a**) that has a PMe_3 ligand and a benzylidene moiety (*anti*-isomer with the phenyl group pointed away from the Cp^* ligand).²⁹ Similarly, thermolysis of **2b** in the presence of PMe_3 at 40 °C for 25 h provided a benzylidene complex $\text{Ta}(\text{=CHPh})\text{Cp}(\eta^4\text{-C}_4\text{H}_6)(\text{PMe}_3)$ (**3b**), which decomposed readily during attempted isolation. Thus, the complex **3b** was characterized in solution by its ^1H NMR spectrum, which exhibited a doublet, characteristic of an α -benzylidene proton, at δ 10.52 ($J_{\text{H-P}} = 5.9$ Hz), downfield from that of **3a** (δ 9.67).

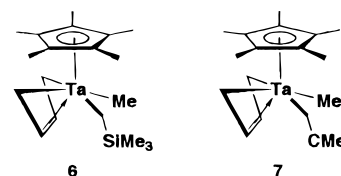


Reaction of **1a** with $\text{Me}_3\text{SiCH}_2\text{MgCl}$ and $\text{Me}_3\text{CCH}_2\text{-MgCl}$ in THF resulted in the formation of monoalkylated complexes $\text{TaCl}(\text{CH}_2\text{SiMe}_3)\text{Cp}^*(\eta^4\text{-C}_4\text{H}_6)$ (**4**) and $\text{TaCl}(\text{CH}_2\text{CMe}_3)\text{Cp}^*(\eta^4\text{-C}_4\text{H}_6)$ (**5**); however, no dialkylated complex was obtained due to the steric bulkiness of the Cp^* ligand and of these Grignard reagents. A similar monophenylated complex $\text{TaCl}(\text{Ph})\text{Cp}^*(\eta^4\text{-C}_4\text{H}_6)$ has been prepared by the reaction of $\text{TaCl}_2\text{Cp}^*(\eta^4\text{-C}_4\text{H}_6)$ with phenyl Grignard reagent.²⁷ The monoalkylated complexes **4** and **5** reacted readily with 1 equiv of methyl Grignard reagent, forming oily products $\text{TaMe}(\text{CH}_2\text{-SiMe}_3)\text{Cp}^*(\eta^4\text{-C}_4\text{H}_6)$ (**6**) and $\text{TaMe}(\text{CH}_2\text{CMe}_3)\text{Cp}^*(\eta^4\text{-C}_4\text{H}_6)$ (**7**), respectively. Since complexes **6** and **7** could not be isolated as pure forms, we determined their structures on the basis of ^1H NMR spectral data: a singlet at -0.45 ppm being attributed to the methyl group bound to the tantalum atom along with a set of signals due to trimethylsilylmethyl or neopentyl groups in the right integral ratio. The asymmetry of the tantalum atom in the complexes **6** and **7** resulted in the six different signals due to the six protons of the coordinated butadiene moiety. All attempts to prepare alkylidene complexes by the thermolysis of **6** and **7** with

Chart 1



or without the donor ligand PMe_3 failed; however, they were found to be catalyst precursors for the ROMP of norbornene, indicating that the formation of an alkylidene species, via a methane-producing α -hydrogen abstraction, proceeded under the polymerization conditions.



From *o*-Xylylene Complexes. A dibenzyl complex $\text{Ta}(\text{CH}_2\text{Ph})_2(\eta^4\text{-}o\text{-(CH}_2)_2\text{C}_6\text{H}_4)\text{Cp}^*$ (**9**), which has an *o*-xylylene auxiliary ligand instead of the η^4 -butadiene, is expected to be a catalyst precursor for the ROMP of norbornene, so we started by preparing the *o*-xylylene complex $\text{TaCl}_2(\eta^4\text{-}o\text{-(CH}_2)_2\text{C}_6\text{H}_4)\text{Cp}^*$ (**8**). Treatment of TaCl_4Cp^* with 1 equiv of $o\text{-C}_6\text{H}_4(\text{CH}_2\text{MgCl})_2$ in THF resulted in the formation of **8** in 38% yield.

Although three coordination modes (**A**, **B**, and **C**, Chart 1) for a mononuclear *o*-xylylene complex are possible, **A** and **B** can be ruled out by NMR spectroscopy.³⁰ Thus the ^1H NMR spectrum of **8** displayed an AB_q-type signal due to the benzylic protons of the *o*-xylylene ligand; this together with signals due to aromatic ring protons at normal chemical shift ruled out the mode **A**. In the ^{13}C NMR spectrum we obtained direct information to distinguish the modes **B** and **C**, a signal due to the benzylic carbons of the *o*-xylylene ligand being displayed at δ 69.9 with a normal coupling constant (142 Hz) for $J_{\text{C-H}}$. The chemical shift values are comparable to that of the known benzyl complexes of tantalum, e.g., **2a** (δ 70.6, 117 Hz), $\text{Ta}(\text{CH}_2\text{Ph})_2(\text{=CHPh})\text{Cp}^*$ (**10**) (δ 71.8, 120 Hz),³¹ $\text{TaCl}_2(\text{CH}_2\text{Ph})_2\text{Cp}^*$ (δ 97.3, 123 Hz),³¹ $\text{TaCl}_2(\text{CH}_2\text{CMe}_3)(\text{CH}_2\text{Ph})\text{Cp}$ (*cis*-isomer: δ 96, 126 Hz; *trans*-isomer: δ 98.6, 128 Hz),³² and $\text{TaCl}_3(\text{CH}_2\text{Ph})_2(\text{PMe}_3)_2$ (δ 82; 133 Hz),³³ except for the highly shielded complex of $\text{Ta}(\text{=CHPh})(\text{CH}_2\text{Ph})\text{Cp}_2$ (**11**) (δ 28.2, 123 Hz).³⁴ The coupling constant (142 Hz) of the benzylic carbons in **8** is larger than those (120–133 Hz) found for other benzyl complexes of tantalum,^{31–34} indicating that the structure of **8** can be best described as mode **C** with some contribution of mode **B**. This is the case with other *o*-xylylene complexes of early transition metals, e.g., Ti, Nb, and W.^{35–39} Thus,

(30) McGrady, J. E.; Stranger, R.; Brown, M.; Bennett, M. A. *Organometallics* **1996**, 15, 3109, and references therein.

(31) Messerle, L. W.; Jennische, P.; Schrock, R. R.; Stucky, G. J. *Am. Chem. Soc.* **1980**, 102, 6744.

(32) Wood, C. D.; McLain, S. J.; Schrock, R. R. *J. Am. Chem. Soc.* **1979**, 101, 3210.

(33) Rupprecht, G. A.; Messerle, L. W.; Fellmann, J. D.; Schrock, R. R. *J. Am. Chem. Soc.* **1980**, 102, 6236.

(34) Schrock, R. R.; Messerle, L. W.; Wood, C. D.; Guggenberger, L. J. *J. Am. Chem. Soc.* **1978**, 100, 3793.

(35) Lappert, M. F.; Raston, C. L.; Skelton, B. W.; White, A. H. *J. Chem. Soc., Chem. Commun.* **1981**, 485.

(36) Lappert, M. F.; Raston, C. L.; Skelton, B. W.; White, A. H. *J. Chem. Soc., Dalton Trans.* **1984**, 893.

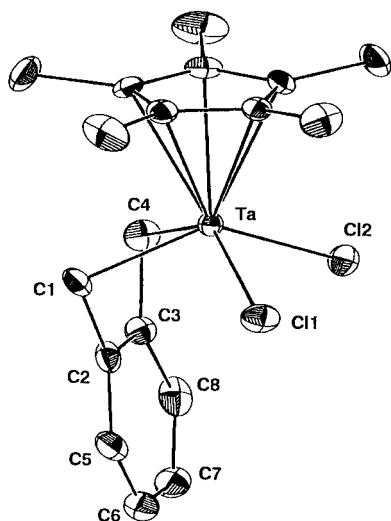
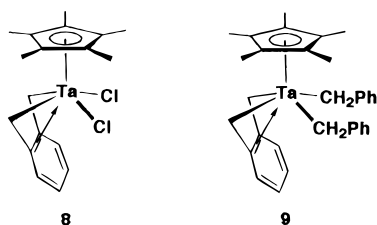


Figure 2. ORTEP drawing of **8** with numbering scheme. Hydrogen atoms are omitted for clarity.

Table 1. Selected Bond Distances (Å) and Angles (deg) of **8**

Bond Distances (Å)			
Ta–Cl(1)	2.400(2)	Ta–Cl(2)	2.405(2)
Ta–C(1)	2.221(8)	Ta–C(2)	2.584(8)
Ta–C(3)	2.578(8)	Ta–C(4)	2.220(8)
Ta–C(11)	2.448(8)	Ta–C(12)	2.448(8)
Ta–C(13)	2.445(8)	Ta–C(14)	2.420(8)
Ta–C(15)	2.419(8)	C(1)–C(2)	1.51(1)
C(2)–C(3)	1.41(1)	C(3)–C(4)	1.49(1)
Bond Angles (deg)			
Cl(1)–Ta–Cl(2)	89.53(9)	Cl(1)–Ta–C(1)	83.8(3)
Cl(1)–Ta–C(4)	138.2(2)	Cl(2)–Ta–C(1)	137.9(2)
Cl(2)–Ta–C(4)	84.1(3)	C(1)–Ta–C(4)	74.1(3)
Ta–C(1)–C(2)	85.5(5)	Ta–C(4)–C(3)	85.7(5)
C(1)–C(2)–C(3)	113.7(8)	C(2)–C(3)–C(4)	116.5(8)

the ^1H and ^{13}C NMR evidence, along with the crystallographic study (vide infra), designated bonding mode **C** for the structure of **8**.



Slow cooling of a toluene solution of **8** provided single crystals suitable for an X-ray diffraction study. An ORTEP drawing of **8** is shown in Figure 2, and the selected bond distances and angles are summarized in Table 1. The coordination of the tantalum atom can be described as the four-legged piano stool geometry comprised of the Cp^* ligand, two C_α atoms of the *o*-xylylene ligand, and two chloro ligands. The Ta– C_α distances (2.221(8) and 2.220(8) Å) are comparable to those of a benzyl complex of tantalum **10** (2.188(15) and 2.233(14) Å),³¹ but are slightly shorter than those of **2a** (2.277-

(4) and 2.249(4) Å)²⁹ and **11** (2.30(1) Å).³⁴ The bonding parameters within the *o*-xylylene and the pentamethylcyclopentadienyl ligand are unexceptional. The Ta– C_β distances (2.584(8) and 2.578(8) Å) in the *o*-xylylene ligand are longer than those in butadiene complexes such as **1b** (2.424(11)–2.410(12) Å),⁴⁰ indicating the presence of bonding interaction between Ta and the C_β carbons as observed for various η^4 -*o*-xylylene complexes (modes **B** and **C**) of early transition metals such as Ti, Nb, and W.^{35–39} The fold angle (104.3°) between Ta–C1–C4 and C1–C2–C3–C4 of **8** is larger than those found for **1b** (94.6°)⁴⁰ and is smaller than those found for some of the *o*-xylylene complexes of Ti (109.5° and 129°)^{36,39} and Nb (126°);³⁶ this is in accord with the NMR result, where bonding mode **C** has some contribution from mode **B**.

The dichloro complex **8** reacted readily with 2 equiv of PhCH_2MgCl in THF to give the corresponding dibenzyl complex **9** in 62% yield. Complex **9** is thermally unstable, and its structure was determined by NMR spectroscopy supported by elemental analysis. The ^1H NMR spectrum of **9** displayed two sets of signals assignable to two benzyl ligands and the *o*-xylylene ligand. In the ^{13}C NMR spectrum, the benzylic carbons of the benzyl ligands appeared at δ 79.9 ($^1J_{\text{CH}} = 119$ Hz), while the benzylic carbons of the *o*-xylylene ligand occurred at 68.8 ($^1J_{\text{CH}} = 137$ Hz); here a smaller coupling constant than that found for **8** suggested a larger contribution from mode **C**.

Monitoring the thermolysis of **9** in C_6D_6 at 20 °C by ^1H NMR spectroscopy revealed a smooth α -hydrogen abstraction accompanied by the elimination of toluene, as the benzyldiene complex $\text{Ta}(\text{=CHPh})(\eta^4\text{-}o\text{-(CH}_2)_2\text{C}_6\text{H}_4\text{)-Cp}^*$ (**12**) was formed. Thus, the complex **12** was isolated in 17% yield by thermolysis of **9** at 40 °C for 4 h followed by recrystallization from a mixture of toluene and hexane. The benzyldiene complex **12** is a dark red and extremely air-sensitive crystalline solid, but it can be stored at room temperature under argon for months without decomposition. It is noteworthy that **12** can be isolated without the electron-donating phosphine ligand like the phosphine-free benzyldiene complex **10**,³¹ this is in sharp contrast to the PMe_3 adduct **3a** obtained by the thermolysis of **2a** in the presence of PMe_3 .²⁹ It is initially difficult to rule out a benzyldiene-bridged dinuclear structure, but a crystallographic study finally confirmed a mononuclear structure for **12** (vide infra). The ^1H NMR spectrum of **12** showed a singlet at δ 4.99 due to the α -benzyldiene proton, indicating the presence of a single alkylidene rotamer. The chemical shift value of the alkylidene carbon of **12** is higher shifted than those (around 10 ppm) found for **3**, being a result of shielding by the aromatic ring of the *o*-xylylene unit. In the ^{13}C NMR spectrum, the benzyldiene carbon atom appeared at δ 230.8 with a coupling constant $J_{\text{C-H}} = 85$ Hz. This chemical shift is comparable to that found for **10** (δ 220, $J_{\text{C-H}} = 82$ Hz)³¹ and otherwise is smaller than those of the corresponding carbon atoms in related complexes, **3a** (δ 237.3, $J_{\text{C-H}} = 112$ Hz, $J_{\text{C-P}} = 19$ Hz) and **11** (δ 246, $J_{\text{C-H}} = 127$ Hz).³⁴ The small coupling constant of **12** is consistent with the large Ta– C_α – C_β

(37) Bristow, G. S.; Lappert, M. F.; Martin, T. R.; Atwood, J. L.; Hunter, W. F. *J. Chem. Soc., Dalton Trans.* **1984**, 399.

(38) Mena, M.; Royo, P.; Serrano, R.; Pellinghelli, M. A.; Tiripicchio, A. *Organometallics* **1988**, 7, 258.

(39) Mena, M.; Royo, P.; Serrano, R.; Pellinghelli, M. A.; Tiripicchio, A. *Organometallics* **1989**, 8, 476.

(40) Yasuda, H.; Tatsumi, K.; Okamoto, T.; Mashima, K.; Lee, K.; Nakamura, A.; Kai, Y.; Kanehisa, N.; Kasai, N. *J. Am. Chem. Soc.* **1985**, 107, 2410.

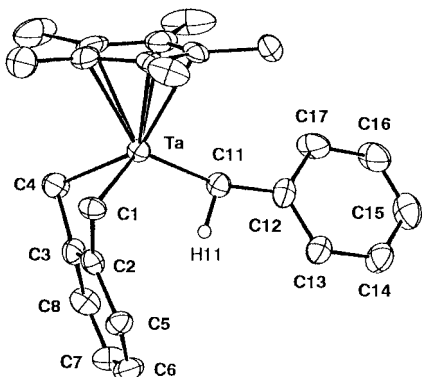


Figure 3. ORTEP drawing of **12** with numbering scheme. Hydrogen atoms except one bound to the carbenic carbon are omitted for clarity.

Table 2. Selected Bond Distances (Å) and Angles (deg) of **12**

Bond Distances (Å)			
Ta–C(1)	2.180(9)	Ta–C(2)	2.572(8)
Ta–C(3)	2.59(1)	Ta–C(4)	2.169(8)
Ta–C(11)	1.925(9)	Ta–C(21)	2.445(9)
Ta–C(22)	2.419(8)	Ta–C(23)	2.415(8)
Ta–C(24)	2.44(1)	Ta–C(25)	2.416(8)
C(1)–C(2)	1.47(1)	C(2)–C(3)	1.42(1)
C(2)–C(5)	1.43(1)	C(3)–C(4)	1.50(1)
C(11)–C(12)	1.49(1)		
Bond Angles (deg)			
C(1)–Ta–C(4)	83.0(4)	C(1)–Ta–C(11)	114.6(4)
C(4)–Ta–C(11)	108.7(4)	Ta–C(1)–C(2)	87.3(5)
Ta–C(4)–C(3)	87.8(5)	Ta–C(11)–C(12)	164.8(7)
C(1)–C(2)–C(3)	120.4(9)	C(2)–C(3)–C(4)	119(1)

angle (vide infra), as expected by the relationship between the M–C–C bond angle in alkylidene complexes and the ^1H – ^{13}C coupling constant for the α -carbon atom.¹

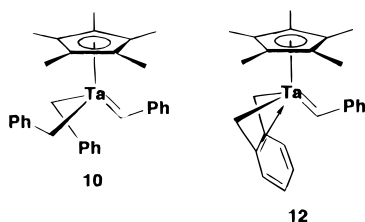


Figure 3 shows an ORTEP drawing of **12**, and selected bond distances and angles are summarized in Table 2. Complex **12** has 16 valence electrons and has a three-legged piano stool geometry comprised of C(1), C(4), and C(11). The structural features of **12** are closely related to the Schrock complex **10**, which also has a three-legged piano stool geometry: two benzyl groups and one benzylidene moiety, the difference is the "up" and "down" orientations of the two benzyl ligands in **10**.³¹ The Ta–C(11) bond distance (1.925(9) Å) is much shorter than that of **3a** (2.044(8) Å)²⁹ and **11** (2.07(1) Å),³⁴ but longer than that (1.883(14) Å) of **10**.³¹ The Ta–C $_{\alpha}$ bond distances (2.169(8) and 2.180(9) Å) of the *o*-xylylene ligand are slightly shorter than those (2.188–(15)–2.233(14) Å) found for the benzyl ligands in **10**.³¹ The *o*-xylylene ligand is sterically more demanding than the Cp* ligand, and so the phenyl group of the benzylidene ligand in **12** points up "toward" the Cp* ligand, i.e., the same, *syn*, direction as that observed in **10**,³¹ but in sharp contrast to the *anti*-geometry found for

benzylidene complexes of group 5 metals having a half-metallocene fragment, e.g., **3a**²⁹ and Cp*M(N-2,6-*i*-Pr₂C₆H₃)(=CHPh)(PMe₃) (**13a**, M = V;⁴¹ **13b**, M = Nb⁴²). The large Ta–C(11)–C(12) angle of 164.8(7)° is almost the same as that (166.0°) found for **10** and is consistent with the small ^1H – ^{13}C coupling constant for the α -carbon atom.

Polymerization of Norbornene. The isolated benzylidene–phosphine complexes **3a** and **3b** did not have any catalytic activity for the ROMP of norbornene, presumably due to the presence of the phosphine ligand, which severely prevents norbornene coordination at the tantalum center. Phosphine-free carbene species, generated in situ from thermolysis of dialkyl complexes **2**, **6**, **7**, and **9**, together with the phosphine-free benzylidene complex **12** can initiate the polymerization of norbornene, and the results are summarized in Table 3. The activity of these precursors depends crucially on the temperature since heating is required to generate the "carbene species" by thermal decomposition, and at higher temperature the yield of the polymer increased to some extent. Higher molecular mass polymers were formed with neat monomer. The stereoselectivity of the reaction, in terms of the polymers' *cis*/*trans* ratio, can be controlled by changing the ancillary ligands (Cp or Cp*, butadiene, or *o*-xylylene) on the tantalum center.

Several notable features of the polymerization reaction can be pointed out. (1) The catalyst precursors **2a**, **6**, and **7**, which have both Cp* and butadiene ligands, gave 97–99% *cis*-polymers. The catalyst precursor **2a** (Table 3, runs 1–7) was superior to **6** and **7** (runs 8–11) in the ROMP of norbornene in that the latter two precursors resulted in a low chemical yield (12–22% yield after 50 h) and larger polydispersity (M_w/M_n 3.25–4.67); however the reactions were highly stereoselective (*cis* content 97–98%). These findings indicated that the benzylidene species was generated from **2a** much more readily than the alkylidenes from **6** and **7**, which requires the release of methane. (2) The Cp complexes **2b** showed no stereoselectivity in double-bond formation (runs 12 and 13), indicating that the Cp and butadiene ligands on the tantalum atom exert similar steric effects. In this context the isoelectronic and analogous "Cp₂Ti=CHR" species has been reported to catalyze the ROMP of norbornene to give poly(norbornene) without any stereoselectivity.^{7,8} (3) In sharp contrast to this high *cis* stereoselectivity, the *o*-xylylene complex **9** gave polymers with 92–95% *trans* double bonds (runs 14–18). The isolated benzylidene complex **12** also initiated the ROMP of norbornene (run 19) with almost the same results as when using the complex **9**. (4) The different stereochemistry of the polymers derived from the butadiene complex and the *o*-xylylene complex is attributed to the significantly larger bulk of the latter ligand and in nonbonded repulsions which are manifest in the different geometry of the rotamers of the initiating alkylidene species, in accordance with the structural features of **3a**²⁹ and **12**.

Hydrogenation of Poly(norbornene). To determine the stereoregularity of the various poly(nor-

(41) Buijink, J. K.; Teuben, J. H.; Kooijman, H.; Spek, A. L. *Organometallics* **1994**, *13*, 2922.

(42) Cockcroft, J. K.; Gibson, V. C.; Howard, J. A. K.; Poole, A. D.; Siemeling, U.; Wilson, C. *J. Chem. Soc., Chem. Commun.* **1992**, 1668.

Table 3. Polymerization of Norbornene Catalyzed by Butadiene Complexes 2a, 2b, 6, and 7 and *o*-Xylylene Complexes 9 and 12

run	compd	temp (°C)	solv	S/C ^a	time (h)	yield ^b (%)	<i>M_n</i> ^c	<i>M_w</i> / <i>M_n</i> ^c	<i>cis</i> ^d (%)
1	2a	45	toluene	100	50	30	4000	2.36	97
2	2a	45	THF	100	50	35	4100	2.00	97
3	2a	45	toluene	100	100	54	5600	1.93	98
4	2a	45	THF	100	100	60	5200	1.92	98
5	2a	65	toluene	100	30	84	8900	1.63	97
6	2a	65	THF	100	30	94	8600	1.88	97
7	2a	65	none	1000	87	43	32 300	2.04	99
8	6	60	toluene	100	50	13	2700	3.25	97
9	6	60	THF	100	50	12	3300	4.05	98
10	7	65	toluene	100	50	14	2100	3.30	98
11	7	65	THF	100	50	22	2600	4.67	97
12	2b	60	toluene	100	32	42	3400	2.46	50
13	2b	60	THF	100	32	16	1800	2.32	50
14	9	45	toluene	100	30	14	2000	1.72	8
15	9	45	THF	100	30	5	5800	2.00	5
16	9	65	THF	100	6	12	3700	1.49	7
17	9	50	none	500	15	6	22 300	1.85	7
18	9	50	none	100	30	73	20 300	1.91	7
19	12	65	toluene	100	30	8	2800	2.13	10

^a S/C: the ratio of norbornenes/catalyst. ^b Methanol-insoluble fraction. ^c GPC analysis in THF versus polystyrene standards. Theoretical *M_n* value is less than the experimental one.⁷ ^d Stereochemistry of double bonds in polymer as determined by ¹H NMR.^{7,8,50}

Table 4. Hydrogenation of Poly(norbornene)s Derived from Polymers Formed Using Complexes 2a and 9 as Catalyst Precursors^a

run	complex	temp (°C)	solv	yield ^b (%)	<i>M_n</i> ^c	<i>M_w</i> / <i>M_n</i> ^c	<i>cis</i> ^d (%)	<i>m</i> ^e (%)
1	2a	65	THF	64	12 000	1.49	97	57
2	2a	65	toluene	67	12 000	1.496	98	55
3	9	50	none	23	19 000	2.34	5	57

^a The ratio of [norbornenes]/[catalyst] was 100. Each polymerization was quenched after 30 h. ^b Methanol-insoluble fraction. ^c GPC analysis in THF versus polystyrene standards. Theoretical *M_n* value is less than the experimental one.⁷ ^d Stereochemistry of double bonds in polymer as determined by ¹H NMR.^{7,8,50} ^e Overall tacticity of hydrogenated form of the polymer expressed as % isotactic (*m*) junctions as determined from its hydrogenated derivative.

bornene)s, we carried out a hydrogenation of the double bonds using diimine generated in situ from *p*-toluene-sulfonylhydrazide (see the Experimental Section),²⁶ and thus we obtained the hydrogenated product in almost quantitative yield. The fully hydrogenated polymers were soluble in CDCl₃ at 50 °C, and high-quality ¹³C NMR spectra for three samples were obtained for estimation of the relative proportions of dyad and triad structures.²⁶ The results for these hydrogenated polymers are shown in Table 4. The poly(norbornene)s that were obtained using the catalyst precursors **2a** and **9** were high *cis* and high *trans*, respectively, and *atactic*, presumably as a result of the monomer adding to the metastable Ta species without any face selectivity. This result however was not expected because the high-*cis* polymers formed from *anti*-7-methylnorbornene using **2a** were 88% *isotactic*.²⁹ Although the reasons for this difference are not clear, this is an important observation because it provides further evidence of an apparent tendency for polymers formed from the prototypal norbornene and norbornadiene, with given catalyst systems, to be much less tactic than those of their derivatives.⁴³

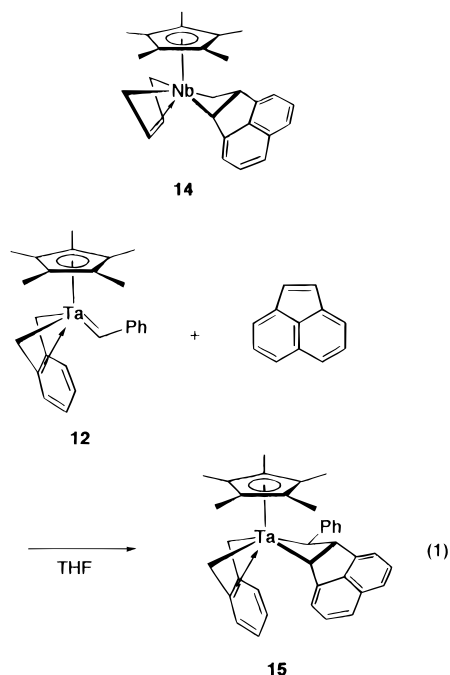
Preparation of a Model Tantalacyclobutane ROMP Intermediate. As mentioned above, norbornene efficiently added to the alkylidene species derived from the tantalum catalyst precursors **3** and **12** to give poly(norbornene), and so it is not surprising that all attempts to isolate a metallacyclobutane, regarded as an intermediate in the propagation of ROMP,² failed.

However acenaphthylene is a cyclic olefin that is expected to react with the alkylidene species to form a metallacyclobutane, and furthermore C–C bond fission is prevented compared with the metallacyclobutane derived from the addition of norbornene. We have in fact successfully isolated and spectroscopically characterized the acenaphthylene adduct of niobium, Cp*(η⁴-butadiene)Nb[CH₂CH(C₁₀H₆)CH] (**14**), which was found to have only a low activity in the ROMP of norbornene.⁴⁴ Thus we investigated reactions of the bis(benzyl) complexes **2**, **6**, **7**, and **9** along with the benzylidene complexes **3** and **12** with a small excess of acenaphthylene under thermal conditions where a benzylidene species is generated. In the reactions of **2**, **3**, **6**, **7**, and **9**, we could not detect any metallacycles at all, and only decomposed products were detected by NMR spectroscopy. On the other hand, the reaction of the complex **12** with acenaphthylene gave rise to a deep violet tantalacyclobutane Cp*(η⁴-*o*-xylylene)Ta[CH(Ph)CH(C₁₀H₆)CH] (**15**) in 18% yield (eq 1), which is air stable in solid form, but decomposed readily in solution upon exposure to air. The formation of **15** in the reaction of **9** with acenaphthylene was detected by NMR spectroscopy, but **15** could not be isolated.

The structure of **15** was determined by ¹H and ¹³C NMR spectroscopy as well as X-ray crystallographic analysis (vide infra). In the ¹H NMR spectrum of **15**, a signal at δ 2.14 due to a β-hydrogen atom, which is

(43) Amir-Ebrahimi, V.; Corry, D. A. K.; Hamilton, J. G.; Rooney, J. J. *J. Mol. Catal.*, in press.

(44) Mashima, K.; Kaidzu, M.; Nakayama, Y.; Nakamura, A. *Organometallics* **1997**, *16*, 1345.



benzylic to the acenaphthylene moiety, was observed. This is at lower field compared with that (δ 1.46) of **14**⁴⁴ and is at lower field than those found for $\text{Cp}^*(\eta^4\text{-C}_4\text{H}_6)\text{Nb}[\text{CH}_2\text{CH}(\text{C}_5\text{H}_8)\text{CH}]$ (**16**) (δ -1.69),⁴⁴ $\text{Cp}_2\text{Ti}[\text{CH}_2\text{-CH}(\text{C}_5\text{H}_8)\text{CH}]$ (**17**) (δ 0.14),⁷ and $(\text{DIPP})_3\text{Ta}[\text{CH}(\text{t-Bu})\text{-CH}(\text{C}_5\text{H}_8)\text{CH}]$ (**18**) (DIPP = 2,6-di(isopropyl)phenoxy) (δ 0.88).⁴⁵ The orientation of the phenyl group on the cyclobutane ring system could not be probed by ^1H NMR experiments, but its *trans* orientation with respect to the acenaphthylene moiety can be determined by the X-ray analysis (vide infra) and is thus consistent with the small geminal coupling constants observed for the α -hydrogen atoms (δ 3.17, $J = 7.9$ Hz and 4.12, $J = 7.7$ Hz). The assignment of the ^{13}C NMR signals to C_α (δ 89.7 and 92.1) and C_β (δ 20.6, $J_{\text{CH}} = 139$ Hz) in the tantalacyclobutane was possible by way of a ^1H - ^{13}C COSY experiment and comparison with those of **14** (C_α , δ 74.1 and 111.6; C_β , δ 20.7, $J_{\text{CH}} = 145$ Hz).⁴⁴ The chemical shift values (δ 63.6 and 64.0) and coupling constants (139 and 140 Hz) for benzylic carbons of the *o*-xylylene ligand are normal and comparable to those found for **8**, **9**, and **12**; the coupling constants suggest a conventional *o*-xylylene ligand with a large contribution of the canonical form **C** in Chart 1.

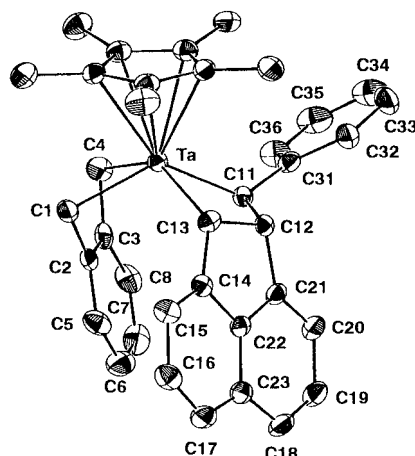
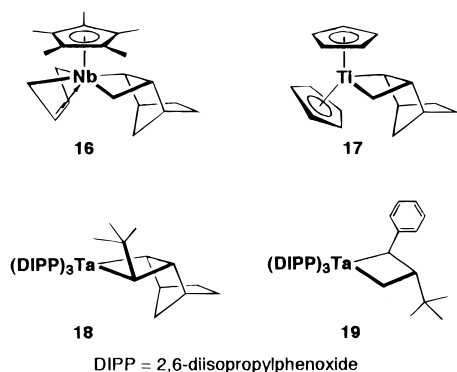


Figure 4. ORTEP drawing of **15** with numbering scheme. Hydrogen atoms are omitted for clarity.

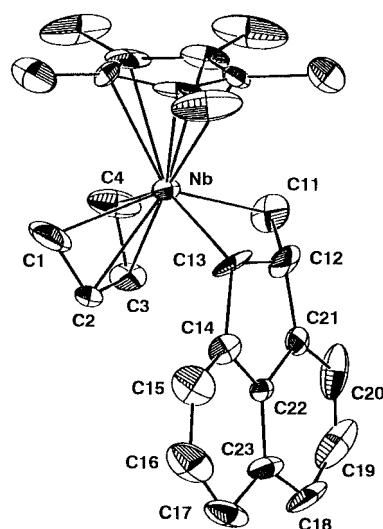


Figure 5. ORTEP drawing of **14** with numbering scheme. Hydrogen atoms are omitted for clarity.

Figure 4 shows the solid-state structure of **15**, and selected bond distances and angles are shown in Table 5. Complex **15** has a four-legged piano stool geometry composed of a capping Cp^* ligand with four carbon atom legs, C(1), C(4), C(11), and C(13), and has a puckered metalacyclobutane structure with a phenyl group at C(11) *trans* to the acenaphthylene ring. This confirms that the addition of acenaphthylene to the $\text{Ta}=\text{C}$ bond of **12** proceeded in the fashion shown to minimize the steric interaction between the Cp^* ligand and the approaching acenaphthylene; the "*syn*" orientation of the " $\text{Ta}=\text{CHPh}$ " moiety in **12** has been retained during addition reaction. The fold angle of 12.5° between $\text{Ta}-\text{C}(11)-\text{C}(13)$ and $\text{C}(11)-\text{C}(12)-\text{C}(13)$ is smaller than that of **16** (29.6°) and those of the tantalacyclobutane

complexes **18**⁴⁵ and $(\text{DIPP})_3\text{Ta}[\text{CH}(\text{Ph})\text{CH}(\text{t-Bu})\text{CH}_2]$ (**19**) (DIPP = 2,6-di(isopropyl)phenoxy), which are 15.5° and 25.2° , respectively.^{45,46} The rather small fold angle of **15** might be attributed to steric congestion caused by the Cp^* and the *o*-xylylene ligands together with the added acenaphthylene moiety. The distance (2.637(6)

(45) Wallace, K. C.; Dewan, J. C.; Schrock, R. R. *Organometallics* **1986**, *5*, 2162.

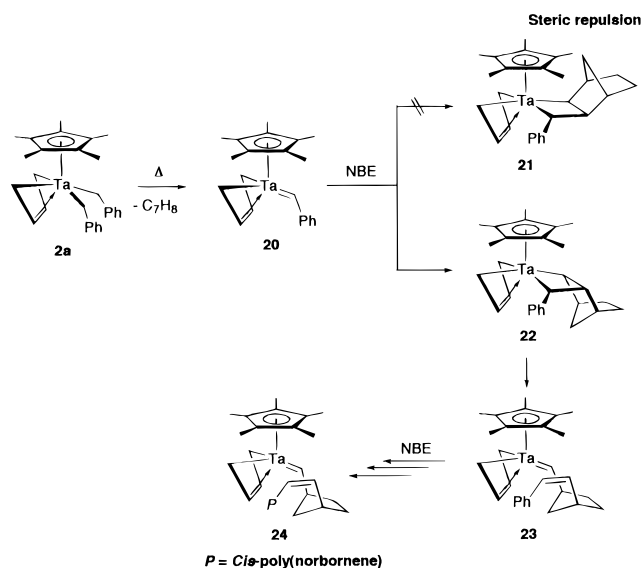
(46) Wallace, K. C.; Liu, A. H.; Dewan, J. C.; Schrock, R. R. *J. Am. Chem. Soc.* **1988**, *110*, 4964.

Table 5. Selected Bond Distances (Å) and Angles (deg) of **14 and **15****

	14 (M = Nb)	15 (M = Ta)
Bond Distances (Å)		
M–C(1)	2.18(3)	2.212(7)
M–C(2)	2.34(2)	2.582(6)
M–C(3)	2.33(2)	2.611(6)
M–C(4)	2.28(2)	2.228(7)
M–C(11)	2.28(2)	2.224(6)
M···C(12)	2.40(2)	2.637(6)
M–C(13)	2.18(1)	2.199(6)
C(1)–C(2)	1.38(3)	1.470(9)
C(2)–C(3)	1.38(3)	1.415(9)
C(3)–C(4)	1.40(3)	1.46(1)
C(11)–C(12)	1.65(3)	1.577(8)
C(12)–C(13)	1.56(3)	1.614(9)
C(11)–C(31)		1.463(9)
Bond Angles (deg)		
C(1)–M–C(4)	71(1)	72.8(3)
C(11)–M–C(13)	80.6(9)	73.9(2)
C(1)–M–C(11)	134(1)	128.4(2)
C(1)–M–C(13)	101(1)	88.6(3)
C(4)–M–C(11)	74(1)	89.7(3)
C(4)–M–C(13)	133.7(9)	139.4(3)
M–C(1)–C(2)	78(2)	86.6(4)
M–C(4)–C(3)	74(1)	87.6(4)
M–C(11)–C(12)	73(1)	86.0(4)
M–C(13)–C(12)	77(1)	86.1(3)
M–C(13)–C(14)	131(1)	136.1(5)
C(1)–C(2)–C(3)	116(3)	114.1(6)
C(2)–C(3)–C(4)	115(2)	115.1(6)
C(11)–C(12)–C(13)	127(2)	112.8(5)
C(11)–C(12)–C(21)	107(2)	111.2(5)
C(12)–C(13)–C(14)	104(2)	105.4(5)
C(12)–C(11)–C(14)		128.5(5)
C(12)–C(11)–C(14)		119.7(6)

Å) of Ta···C(12) in **15** is longer than the corresponding distances found for **16** (2.44(1) Å) and **18** (2.382(16) Å), but is shorter than that (2.782(24) Å) of **19**. The bond distance (2.224(6) Å) of Ta–C(11) is longer than that (2.199(6) Å) of Ta–C(13), although both C(11) and C(13) are benzylic carbons, presumably due to the presence of the acenaphthylene ring system. The angles of C(1)–Ta–C(4) (72.8(3)°) and C(11)–Ta–C(13) (73.9(2)°), which are of chelating ligands, are smaller than the angles of C(1)–Ta–C(13) (88.6(3)°) and C(4)–Ta–C(11) (89.7(3)°). The *o*-xylylene ligand of **15** is bending away to minimize the congestion between the metallacyclic moiety and the *o*-xylylene ligand; the fold angle (98.7°) between the plane of Cp ring carbons and the plane of C(1)–C(2)–C(3)–C(4) is larger than that of **8** (80.7°) and **12** (81.9°).

The tantallacyclic ring system of **15** is essentially the same as the structure of the niobacyclic ring system of **14** except for the absence of the phenyl group in the ring system of **14**. The structure of **14** is of poor quality, and thus the accuracy of bond parameters of **14** is limited. Selected bond distances and angles of **14** are listed in Table 5, and a drawing of **14** is provided in Figure 5. **14** may be described as having a four-legged piano stool geometry composed of a capping Cp* ligand and four carbon atom legs, C(1), C(4), C(11), and C(13), with a metallacyclobutane geometry that is almost flat (the fold angle of Ta–C(11)–C(13) and C(11)–C(12)–C(13) = 2.8°). The Nb···C(12) distance of 2.40(2) Å was shorter than that of **15**. The tendency of a longer Nb–C(11) (2.28(2) Å) and a shorter Nb–C(13) (2.18(1) Å) is comparable to that found for **15**.

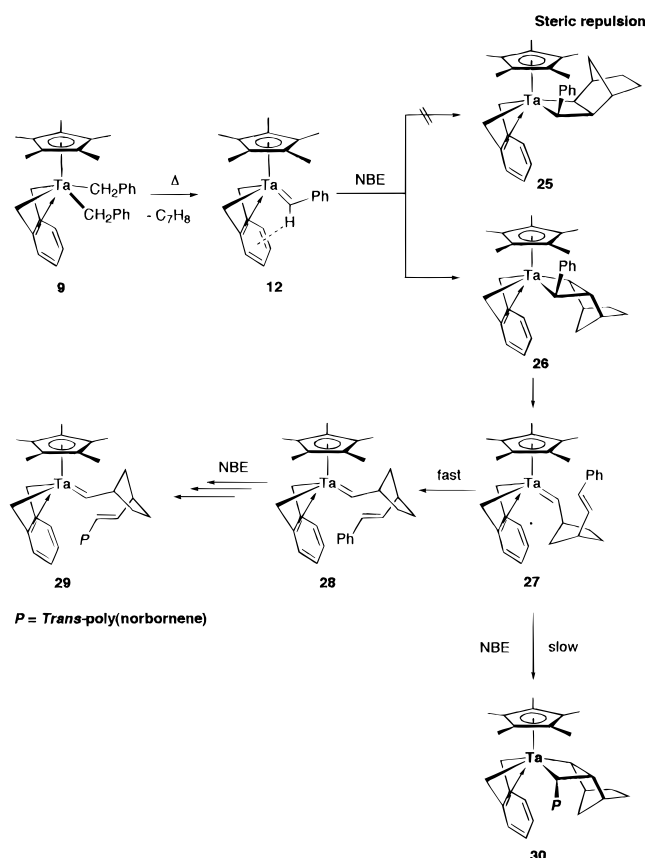
Scheme 1

Mechanistic Outline. To understand the factors that determine the stereochemistry of the double bonds in poly(norbornene) and the high *cis*/*trans* stereoselectivity and poor stereoregularity (almost *atactic*), we isolated two benzylidene complexes, **3a** and **12**, which can be regarded as key intermediates in the ROMP catalyzed by our tantalum catalyst system. **3a** has an *anti*-benzylidene ligand, while **12** is *syn*, and it is expected that the stability of the rotamer of the alkylidene species during the propagation will control the stereochemistry of the double bond of poly(norbornene) because *syn*- and *anti*-rotamers of molybdenum complexes of the type Mo(NAr)(=CHMe₂Ph)(OR)₂ (Ar = 2,6-Me₂C₆H₃, 2,6-*i*-Pr₂C₆H₃; OR = O-*i*-Bu, OMe(CF₃)₂, etc.) have been demonstrated to play a major role in determining whether certain other polymers contain *cis* or *trans* double bonds.^{12,17} With the butadiene complex **2a** as a catalyst precursor, the relative geometry of the alkylidene species, and presumably the propagating chain end of the polymer, is mostly *anti* (see **20**, **23**, and **24** in Scheme 1). On the other hand, the *o*-xylylene ligand is much more sterically demanding than the butadiene ligand and thus induces the formation of a metastable *anti*-alkylidene species **27** (see Scheme 2). The formation of *syn*-**28** and -**29**, similar to **12** (as shown in Scheme 2), seems to be taking place, although this could not be detected. Accordingly, we can control the orientation of the rotational isomer by varying an auxiliary ligand, e.g., butadiene or *o*-xylylene, on the tantalum center.

With regard to half-metallocene complexes of group 5 metals **13a**⁴¹ and **13b**,⁴² vide supra, which are isoelectronic to the complex **3a** including the PMe₃ ligand, an “*anti*”-alkylidene ligation is observed. It therefore seems curious that complex **12**, which also has a 14-valence TaCp*(η^4 -*o*-xylylene) fragment isoelectronic to the TaCp*(η^4 -diene) fragment, adopts the *syn*-isomer just like the Schrock complex **10**, which has the *syn*-benzylidene ligand. The *syn*-geometry found for **12** might be attributed to the CH– π interaction as shown in Scheme 2,⁴⁷ and this emphasizes the unique ability

(47) Steiner, T.; Starikov, E. B.; Amado, A. M.; Teixeira-Dias, J. J. C. *J. Chem. Soc., Perkin Trans. 2* **1995**, 1321.

Scheme 2

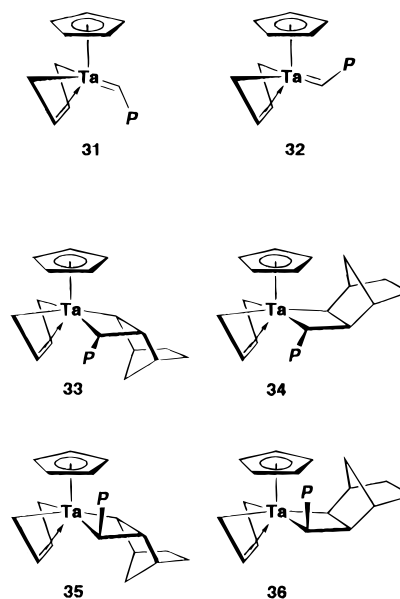


of the *o*-xylylene ligand to control the chain end isomer as opposed to that of the butadiene complex.

Metallacyclobutanes have been demonstrated as intermediates in ROMP. We assume that norbornene approaches the Ta=C bond to minimize the steric repulsion of the Cp* ligand, and this is confirmed by the structural study for niobacyclobutane **14**, where C(7) is pointing away from the Cp* ligand; thereby **21** in Scheme 1 and **25** in Scheme 2 are less favorable products. We can postulate that, in the case of the butadiene complexes (Scheme 1), an “*all-cis*”-metallacycle **22** is likely to be formed, and subsequent ring-opening would then afford a *cis*-double bond and an inserted product **23** along with **24**. For the *o*-xylylene catalysts (Scheme 2), the *trans*-metallacycle **26** is assumed to be the product upon addition of monomer to **12**; the metathesis reaction resulted in the formation of a *trans*-double bond and a new *anti*-alkylidene complex **27** that is expected to isomerize to the *syn*-species such as **28** and **29**. This interconversion seems to be much faster than the addition of monomer to **27**, which would lead to the formation of the “*all-cis*”-metallacycle **30**, which then would give a *cis*-double bond, as shown in Scheme 1. The formation of **30** is unfavorable because there is steric repulsion between the polymer chain end and the *o*-xylylene ligand, but this may explain some contamination of the *cis*-double bonds in the polymer obtained using the *o*-xylylene complexes. Furthermore, it is of interest that the rate of polymer formation catalyzed by the *o*-xylylene precursors is much slower than that of the butadiene catalysts.

It is rather difficult to control the stereochemistry of the C=C bond in poly(norbornene), although many

kinds of functionalized norbornadiene monomers have been polymerized in high stereoselectivity and stereoregularity using metal salt-based catalyst systems,⁴⁰ and recently *all-trans* highly tactic^{10,13} and *all-cis* highly tactic polymers¹⁶ have been obtained by using well-defined molybdenum alkylidene complexes. Complexes **16**⁷ and **18**⁴⁵ are less stereoselective and catalyze the ROMP of norbornene to give 55 and 62% *trans*-poly(norbornene)s, respectively. The successful stereocontrol described in the present study is attributed to the incorporation of the bulky Cp* ligand with auxiliary ligands such as butadiene and *o*-xylylene, and the benefits of these steric effects are emphasized when one considers polymerizations using **2b**, a Cp–butadiene complex, as a catalyst precursor; the resulting poly(norbornene) had a 1:1 mixture of *cis* and *trans*, indicating no stereoselectivity. Although a phosphine complex **3b** was found to be the same *anti*-rotamer as **3a**, two rotamers, **31** and **32**, are likely to be generated during the propagation process. Norbornene may be added to **31** in two different ways to form metallacyclobutanes **33** and **34**, while the addition of norbornene to **32** yields **35** and **36**; subsequent metathesis reaction of these four possible metallacyclobutanes regenerate **31** and **32**, resulting in a nonselective C=C bond formation.



Four possible stereochemical representations of poly(norbornene) are shown in Figure 1; alternating addition of norbornene to each face of the Ta=C bond (single rotamer) affords *syndiotactic* polymer, while the addition to the same face of the Ta=C bond results in *isotactic* polymer. There are only a few known examples of tactic poly(norbornene) in contrast to many examples of tactic polymers made from norbornadiene derivatives; *cis syndiotactic* poly(norbornene) has been obtained using the ReCl₅-based heterogeneous catalyst,²⁶ and a *trans, isotactic-rich* example was also reported.²⁶ Although quite high stereoselectivity for the double bond in the polymer was accomplished with the present tantalum catalyst precursors, the polymers were almost atactic as determined by ¹³C NMR spectroscopy of their hydrogenated derivatives. This result suggests that the alkylidene species would be in a resting state during

the propagation, and thereby the monomer added to both of the faces of the Ta=C bond, leading to the *atactic* polymer.

Conclusion

In this contribution, we demonstrated that *cis*-dialkyl complexes of tantalum bearing an η^5 -C₅R₅ and an auxiliary ligand such as 1,3-butadiene and *o*-xylylene are efficient catalyst precursors for the ROMP of norbornene. The factors governing the unexpectedly high stereoselectivity have been investigated by examining the structures of well-defined alkylidene and metalla-cyclobutane derivatives.

When the Cp*-butadiene complexes **2a**, **6**, and **7** are employed, the main feature of the polymerization system is that high *cis*, *atactic* poly(norbornene) is formed. This is a consequence of (i) the alkylidene-propagating species preferring to exist as the *anti*-rotamer assumed on the basis of the isolation and crystallographic characterization of **3a** and (ii) subsequent *exo*-addition of norbornene to the alkylidene without face selectivity to produce another *anti*-alkylidene and a *cis*-vinylene bond. The stereoselectivity of the reaction depends sensitively on the ligand environment at the catalyst site. For example the Cp-butadiene complex **2b** did not show any stereoselectivity in the ROMP of norbornene, and this is attributed to the similarity of the steric bulk of the Cp and butadiene ligands; therefore, both rotamers are available for propagation. We also found that the *o*-xylylene complexes **9** and **12** catalyzed the ROMP of norbornene to yield high *trans*, *atactic* polymer and that the benzylidene complex **12** was characterized crystallographically to be a *syn*-rotamer, addition of monomer to which affords a *trans*-vinylene bond and an *anti*-rotamer. Fast conversion of the *anti*-rotamer **27** to a *syn*-rotamer **28** is assumed to be the key step in the mechanism.

We could not detect any metallacyclobutanes during the polymerization; however, we isolated and crystallographically characterized an acenaphthylene adduct **15** that suggests *exo*-addition to the Ta=C bond with the retention of the *syn*-geometry.

Experimental Section

General Procedures. All manipulations involving air- and moisture-sensitive organometallic compounds were carried out by use of standard Schlenk techniques under an argon atmosphere. Hexane, THF, toluene, and pentane were dried and deoxygenated by distillation over sodium benzophenone ketyl under argon. Methanol was refluxed over magnesium and distilled under argon. Benzene-*d*₆ was distilled from Na/K alloy and thoroughly degassed by trap-to-trap distillation before use. PMe₃ purchased as toluene solution (1.0 M) from Aldrich Chemical Co., was used as received. Ethylene was purchased from Seitetsu Kagaku Co. and was used as received. Norbornene (bicyclo[2.2.1]hept-2-ene) from the Aldrich was refluxed over sodium and distilled prior to use. Acenaphthylene was sublimed before use. Complexes TaCl₂(η^5 -C₅R₅)(η^4 -buta-1,3-diene) (R = CH₃ (**1a**); R = H (**1b**)) were prepared according to the literature,^{40,48} and the complex Cp*(η^4 -butadiene)Nb[CH₂CH(C₁₀H₆)CH] (**14**) has been reported previously.⁴⁴

The ¹H (500, 400, and 270 MHz) and ¹³C (125, 100, and 68 MHz) NMR spectra were measured on a JEOL JNM-GX500, a JEOL JNM-GSX400, or a JEOL JNM-EX270 spectrometer. When C₆D₆ was used as the solvent, the spectra were referenced to the residual solvent protons at δ 7.20 in the ¹H NMR spectra and to the residual solvent carbons at δ 128.0 (triplet for C₆D₆) in the ¹³C NMR spectra. Assignments for ¹H and ¹³C NMR peaks for some of the complexes were aided by 2D ¹H-¹H NOESY and 2D ¹H-¹³C COSY spectra, respectively. Elemental analyses were performed at Elemental Analysis Center, Faculty of Science, Osaka University. All melting points of the complexes were measured in sealed tubes under argon atmosphere and were not corrected.

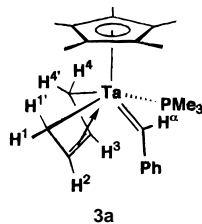
Ta(CH₂Ph)₂(η^5 -C₅Me₅)(η^4 -buta-1,3-diene) (2a**).** To a solution of **1a** (0.592 g, 1.34 mmol) in THF (60 mL) cooled at -78 °C was added an ethereal solution of PhCH₂MgCl (2.11 equiv, 2.84 mmol) via a syringe. The reaction mixture was stirred for 2.5 h at 25 °C. The color of the solution changed from purple to dark red. All volatiles were removed under reduced pressure to give a residue, from which the product was extracted with hexane (120 mL). Recrystallization from toluene (5 mL) at -20 °C afforded **2a** as dark red crystals in 83% yield; mp 121–122 °C (dec). Complex **2a** is thermally unstable, and the content of **2a** was reduced to ca. 10% after 4 days at 25 °C, it also decomposed to about 60% on heating at 45 °C for 6 h. ¹H NMR (270 MHz, C₆D₆, 303 K): δ -0.79, (2H, m, =CH₂ anti), 0.02 (2H, m, =CH₂ syn), 0.40, 1.23 (4H, AB quartet, ²J_{HH} = 10.9 Hz, Ta-CH₂-Ph), 1.77 (15H, s, C₅Me₅), 6.39 (2H, m, =CH-), 6.85 (4H, d, ³J_{HH} = 6.9 Hz, *o*-C₆H₅), 6.94 (2H, t, ³J_{HH} = 7.6 Hz, *p*-C₆H₅), 7.32 (4H, t, ³J_{HH} = 7.6 Hz, *m*-C₆H₅). ¹³C NMR (68 MHz, C₆D₆, 303 K): δ 11.4 (q, ¹J_{CH} = 127 Hz, C₅Me₅), 60.1 (t, ¹J_{CH} = 150 Hz, =CH₂), 70.6 (t, ¹J_{CH} = 117 Hz, Ta-CH₂-Ph), 119.2 (s, C₅Me₅), 120.9 (d, ¹J_{CH} = 169 Hz, =CH-), 122.7 (d, ¹J_{CH} = 157 Hz, *p*-C₆H₅), 126.5 (d, ¹J_{CH} = 156 Hz, *o*-C₆H₅), 127.7 (d, ¹J_{CH} = 154 Hz, *m*-C₆H₅), 153.9 (s, *ipso*-C₆H₅). Anal. Calcd for C₂₈H₃₅Ta: C, 60.87; H, 6.38. Found: C, 60.86; H, 6.37.

Preparation of Ta(CH₂Ph)₂(η^5 -C₅H₅)(η^4 -buta-1,3-diene) (2b**).** To a solution of **1b** (0.198 g, 0.534 mmol) in THF (45 mL) cooled at -78 °C was added a solution of PhCH₂MgCl (2.16 equiv, 1.16 mmol) in ether via a syringe. The color of the reaction solution changed from violet to brown. All volatiles were removed under reduced pressure to give a residue, from which the product was extracted with toluene and hexane (1:10) (100 mL). The solution was concentrated to 3 mL and kept at -20 °C to afford **2b** as brown crystals in 51% yield; mp 108–109.5 °C (dec). Complex **2b** is air and moisture sensitive. ¹H NMR (270 MHz, C₆D₆, 303 K): δ -0.82, (2H, m, =CH₂ anti), 0.07 (2H, m, =CH₂ syn), 1.27 and 1.86 (4H, AB quartet, ²J_{HH} = 10.9 Hz, Ta-CH₂-Ph), 5.79 (5H, s, C₅H₅), 6.69 (2H, m, =CH-), 6.75 (4H, d, ³J_{HH} = 6.9 Hz, *o*-C₆H₅), 6.89 (2H, t, ³J_{HH} = 7.4 Hz, *p*-C₆H₅), 7.27 (4H, t, ³J_{HH} = 7.7 Hz, *m*-C₆H₅). Anal. Calcd for C₂₃H₂₅Ta: C, 57.27; H, 5.22. Found: C, 57.27; H, 5.22.

Preparation of Ta(=CHPh)(η^5 -C₅Me₅)(η^4 -buta-1,3-diene)(PMe₃) (3a**).** To a solution of **2** (0.258 g, 0.47 mmol) in toluene (6.0 mL) was added a solution of PMe₃ (1.07 equiv, 0.50 mmol) in toluene (1.0 M, 0.50 mL) via a syringe at room temperature. The reaction mixture was stirred for 16 h at 48 °C, during which time the color of the solution turned to reddish brown. The solution was concentrated to ca. 3 mL and then was kept at -20 °C to afford **3a** as yellow-brown crystals in 55% yield; mp 113–118 °C (dec). Complex **3a** is air and moisture sensitive both in solid form and in solution and is thermally unstable in hydrocarbon solvents, being decomposed to the extent of about 60% by heating at 60 °C for 24 h. The ¹H and ¹³C NMR were referenced to THF-*d*₈ at δ 3.60 and δ 67.4, respectively. The 2D ¹H-¹H NOESY spectrum displayed among the protons H⁴-PMe₃ (w), Ph ^{α} -H² (w), Ph ^{α} -Cp* (w), Ph ^{α} -PMe₃ (w), H ^{α} -Cp* (m), H¹-H² (s), H⁴-H³ (s), and so on. ¹H NMR (270 MHz, THF-*d*₈, 303 K): δ -1.01 (1H, m, H⁴),

(48) Okamoto, T.; Yasuda, H.; Nakamura, A.; Kai, Y.; Kanehisa, N.; Kasai, N. *J. Am. Chem. Soc.* **1988**, *110*, 5008.

−0.73 (1H, m, H¹), 0.47 (1H, m, H⁴), 1.18 (9H, d, ²J_{HP} = 7.3 Hz, PMe₃), 1.32 (1H, m, H¹), 2.11 (15H, s, C₅Me₅), 5.57 (1H, m, H³), 6.23 (1H, m, H²), 6.59 (1H, t, ³J_{HH} = 7.1 Hz, *p*-C₆H₅), 6.91 (2H, d, ³J_{HH} = 7.6 Hz, *o*-C₆H₅), 7.01 (2H, t, ³J_{HH} = 7.8 Hz, *m*-C₆H₅), 9.67 (1H, d, ³J_{HP} = 5.9 Hz, Ta=CHPh). ¹³C NMR (68 MHz, THF-*d*₆, 303 K): δ 12.5 (q, ¹J_{CH} = 126 Hz, C₅Me₅), 18.4 (qd, ¹J_{CH} = 129 Hz, ¹J_{CP} = 22 Hz, PMe₃), 43.7 (t, ¹J_{CH} = 148 Hz, C⁴), 52.8 (t, ¹J_{CH} = 149 Hz, C¹), 104.2 (d, ¹J_{CH} = 159 Hz, C³), 110.3 (d, ¹J_{CH} = 166 Hz, C²), 110.8 (s, C₅Me₅), 122.5 (d, ¹J_{CH} = 158 Hz, *p*-C₆H₅), 127.7 (d, ¹J_{CH} = 155 Hz, *m*-C₆H₅), 128.7 (d, ¹J_{CH} = 155 Hz, *o*-C₆H₅), 155.2 (s, *ipso*-C₆H₅), 237.3 (dd, ¹J_{CH} = 112 Hz, ²J_{CP} = 19 Hz, Ta=CHPh). ³¹P{H} NMR (109 MHz, THF-*d*₆, 303 K): δ −17.1 (PMe₃). Anal. Calcd for C₂₄H₃₆PTa: C, 53.73; H, 6.76. Found: C, 53.32; H, 6.69.



3a

Preparation of Ta(=CHPh)(η^5 -C₅H₅)(η^4 -buta-1,3-diene)(PMe₃) (3b). Complex **2b** (ca. 6 mg, ca. 0.01 mmol) was dissolved in 0.6 mL of C₆D₆ in a 5 mm NMR tube. To the dark brown solution was added an excess of PMe₃ (ca. 4 μ L, ca. 0.04 mmol) at 25 °C. After the NMR tube was sealed and placed for 25 h in an oil bath heated at 40 °C, the ¹H NMR spectrum was measured. Peaks due to **3b** were observed along with signals due to free toluene (δ 2.15, s, PhCH₃) and excess PMe₃ (δ 0.83, d, ²J_{HP} = 2.3 Hz). ¹H NMR (270 MHz, C₆D₆, 303 K): δ −0.33, 0.27, 0.55 and 1.82 (4H, m, =CH₂), 0.72 (9H, d, ²J_{HP} = 7.6 Hz, PMe₃), 5.54 (5H, s, C₅H₅), 10.52 (1H, d, ³J_{HP} = 5.9 Hz, Ta=CHPh). The resonances of the C₆H₅ and the methine (=CH−) of the butadiene ligand were not assigned because they were overlapped by C₆D₆ and toluene signals. All attempts to isolate **3b** failed.

Preparation of TaMe(CH₂SiMe₃)(η^5 -C₅Me₅)(η^4 -buta-1,3-diene) (6). To a solution of **1a** (0.432 g, 0.98 mmol) in THF (40 mL) cooled at −78 °C was added a solution of Me₃SiCH₂MgCl (1.12 equiv, 1.10 mmol) in ether (0.38 M, 2.90 mL) via a syringe. The reaction mixture was stirred for 5 h at 20 °C, and then a solution of MeMgI (1.02 equiv, 1.00 mmol) in ether (1.11 M, 0.90 mL) was added at −78 °C followed by stirring for 2 h at 20 °C. All volatiles were removed under reduced pressure, and the residue was extracted with pentane (15 mL). The product **6** was very highly soluble in pentane and therefore was not isolated but gave a red-purple oil on solvent removal. ¹H NMR (270 MHz, C₆D₆, 303 K): δ −1.04, −0.77, and 0.06 (3H, m, =CH₂), −1.66 and −0.30 (2H, AB quartet, ²J_{HH} = 12.2 Hz, Ta-CH₂-SiMe₃), −0.45 (3H, s, Ta-CH₃), 0.25 (9H, s, −SiMe₃), 1.78 (15H, s, C₅Me₅), 7.03 (1H, m, =CH−), 7.26 (1H, m, =CH−). One proton resonance (=CHH) of the butadiene ligand was not assigned because of being overlapped by impurity peaks.

Preparation of TaMe(CH₂CMe₃)(η^5 -C₅Me₅)(η^4 -buta-1,3-diene) (7). To a solution of **1a** (0.108 g, 0.24 mmol) in THF (40 mL) cooled at −78 °C was added a solution of Me₃CCH₂MgCl (1.17 equiv, 0.29 mmol) in ether (0.13 M, 2.20 mL) via a syringe. The reaction mixture was stirred for 3 h at 20 °C, and then a solution of MeMgI (1.12 equiv, 0.27 mmol) in ether (0.42 M, 0.65 mL) was added at −78 °C followed by stirring for 2 h at 20 °C. All volatiles were removed under reduced pressure, and the residue was extracted with hexane (25 mL). The extract was concentrated to afford **7** as a dark red-purple oily compound (80% yield). ¹H NMR (270 MHz, C₆D₆, 303 K): δ −1.13, 0.86, and 0.11 (3H, m, =CH₂), −1.27 and 0.17 (2H, AB quartet, ²J_{HH} = 13.4 Hz, Ta-CH₂-CMe₃), −0.45 (3H, s, Ta-CH₃), 1.22 (9H, s, −CMe₃), 1.78 (15H, s, C₅Me₅), 6.90 (1H,

m, =CH−), 7.87 (1H, m, =CH−). One proton resonance (=CHH) of the butadiene ligand was not assigned because of overlap by impurity peaks.

Preparation of Ta(η^5 -C₅Me₅)[*o*-(CH₂)₂C₆H₄]Cl₂ (8). To a solution of Cp*TaCl₄ (0.561 g, 1.23 mmol) in THF (45 mL) cooled at −78 °C was added a suspension of *o*-C₆H₄(CH₂MgCl)₂ (1.2 equiv, 1.47 mmol) in THF (0.21 M, 7.00 mL) via a syringe. The reaction mixture was allowed to warm to room temperature, stirred overnight, and evaporated to dryness. The product was extracted with hot hexane (180 mL) at 60 °C. Recrystallization from toluene (2.5 mL) at −20 °C afforded **8** as red crystals in 38% yield; mp 241.0–243.5 °C (dec). ¹H NMR (270 MHz, C₆D₆, 303 K): δ 0.47 and 1.57 (4H, AB quartet, ²J_{HH} = 7.9 Hz, −CH₂), 1.94 (15H, s, C₅Me₅), 7.52 (4H, m, C₆H₄). ¹³C NMR (100 MHz, C₆D₆, 303 K): δ 12.0 (q, ¹J_{CH} = 128 Hz, C₅Me₅), 69.94 (t, ¹J_{CH} = 142 Hz, −CH₂), 123.9 (s, C₅Me₅), 131.3 and 137.3 (d, ¹J_{CH} = 160 and 161 Hz, respectively, C₆H₄), 127.3 (s, *ipso*-C₆H₄). Anal. Calcd for C₁₈H₂₃Cl₂Ta: C, 44.01; H, 4.72. Found: C, 44.68; H, 4.78.

Preparation of Ta(CH₂Ph)₂(η^5 -C₅Me₅)[*o*-(CH₂)₂C₆H₄] (9). To a solution of **8** (0.199 g, 0.41 mmol) in THF (30 mL) cooled to −78 °C was added an ethereal solution of PhCH₂MgCl (2.3 equiv, 0.92 mmol) via a syringe. The reaction mixture was stirred for 0.5 h at 25 °C, and the color of the solution changed from red to dark red. All volatiles were removed under reduced pressure to give a residue, from which the product was extracted with hexane (50 mL). Recrystallization from toluene (1.5 mL) and hexane (1.0 mL) at −20 °C afforded **9** as dark red crystals in 62% yield; mp 107–108 °C (dec). Complex **9** is thermally unstable and almost completely decomposed after 20 h at 20 °C to give **12**. ¹H NMR (400 MHz, C₆D₆, 303 K): δ 0.26, (2H, br, −CH₂ anti), 0.99 (2H, br, −CH₂ syn), 0.81 and 1.78 (4H, AB quartet, ²J_{HH} = 11.5 Hz, −CH₂-Ph), 1.72 (15H, s, C₅Me₅), 6.69 (4H, d, ³J_{HH} = 7.0 Hz, *o*-C₆H₅), 6.90 (2H, t, ³J_{HH} = 7.3 Hz, *p*-C₆H₅), 6.95 and 7.37 (4H, m, C₆H₄), 7.24 (4H, t, ³J_{HH} = 7.8 Hz, *m*-C₆H₅). ¹³C NMR (100 MHz, C₆D₆, 303 K): δ 11.5 (q, ¹J_{CH} = 128 Hz, C₅Me₅), 68.8 (br t, ¹J_{CH} = 137 Hz, −CH₂), 79.9 (br t, ¹J_{CH} = 119 Hz, −CH₂Ph), 119.5 (s, C₅Me₅), 122.8 (d, ¹J_{CH} = 158 Hz, *p*-C₆H₅), 127.4 (d, ¹J_{CH} = 160 Hz, *m*-C₆H₅), 130.0 and 133.3 (d, ¹J_{CH} = 163 and 156 Hz, respectively, C₆H₄), 129.3 (s, *ipso*-C₆H₄), 152.0 (s, *ipso*-C₆H₅). The resonances of the *o*-C₆H₅ were overlapped by C₆D₆. Anal. Calcd for C₃₂H₃₇Ta: C, 63.78; H, 6.19. Found: C, 63.63; H, 6.10.

Preparation of Ta(=CHPh)(η^5 -C₅Me₅)[*o*-(CH₂)₂C₆H₄] (12). To a solution of **8** (0.294 g, 0.698 mmol) in THF (50 mL) cooled at −78 °C was added PhCH₂MgCl (2.2 equiv, 1.52 mmol) in ether (0.66 M, 2.30 mL) via a syringe. The reaction mixture was warmed to 20 °C, and the color of the solution changed from red to dark red, indicating the formation of **9**. All volatiles were removed under reduced pressure to give a residue, from which the product was extracted with hexane (50 mL). The hexane solution of the product was heated at 40 °C for 9 h. Recrystallization from toluene (2.0 mL) and hexane (2.0 mL) at −20 °C afforded **12** as dark red crystals in 17% yield; mp 257.0–258.5 °C (dec). ¹H NMR (400 MHz, C₆D₆, 303 K): δ −0.07, (2H, d, ²J_{HH} = 12.8 Hz, −CH₂ anti), 1.92 (15H, s, C₅Me₅), 3.49 (2H, d, ²J_{HH} = 12.8 Hz, −CH₂ syn), 4.99 (1H, s, =CHPh), 6.72 (2H, d, ³J_{HH} = 8.2 Hz, *o*-C₆H₅), 6.79 (1H, t, ³J_{HH} = 7.3 Hz, *p*-C₆H₅), 7.09 (2H, m, *m*-C₆H₅), 7.32 and 7.45 (4H, m, C₆H₄). ¹³C NMR (100 MHz, C₆D₆, 303 K): δ 11.6 (q, ¹J_{CH} = 128 Hz, C₅Me₅), 56.1 (t, ¹J_{CH} = 145 Hz, −CH₂), 113.8 (s, C₅Me₅), 118.7 (s, *ipso*-C₆H₄), 122.9 (d, ¹J_{CH} = 158 Hz, *p*-C₆H₅), 127.3 (*m*-C₆H₅), 127.4 (*o*-C₆H₅), 131.1 (d, ¹J_{CH} = 162, C₆H₄), 230.8 (d, ¹J_{CH} = 85 Hz, =CHPh). The resonances of the *ipso*-C₆H₄ and *ipso*-C₆H₅ were overlapped by C₆D₆ and impurity, respectively.

Preparation of Ta[CH(Ph)CH(C₁₀H₆)CH](η^5 -C₅Me₅)[*o*-(CH₂)₂C₆H₄] (15). To a solution of **12** (0.229 g, 0.47 mmol) in THF (40 mL) cooled at −78 °C was added acenaphthylene (83

mg, 0.54 mmol) in 7 mL of THF and PhCH_2MgCl (2.2 equiv, 1.06 mmol) in ether (0.66 M, 1.60 mL) via a syringe. The reaction mixture was allowed to warm to 20 °C, the color of the solution changed from red to dark red, and stirring was continued for 30 h. All volatiles were removed under reduced pressure to give a residue, from which the product was extracted with hexane (170 mL). Recrystallization from toluene (7.0 mL) at -20 °C afforded **15** as dark-red purple crystals in 18% yield; mp 162.0–163.0 °C (dec). ^1H NMR (500 MHz, C_6D_6 , 303 K): δ 0.24, 0.54, 1.25, and 1.48 (4H, d, $^2J_{\text{HH}} = 9.5, 7.7, 7.7$, and 10.3 Hz, respectively, $-\text{CH}_2$ (xylylene)), 2.14 (1H, m, $\beta\text{-H}$), 3.17, 4.12, (2H, d, $^2J_{\text{HH}} = 7.9$ and 7.7 Hz, $\alpha\text{-H}$), 1.64 (15H, s, C_5Me_5), 5.8–7.6 (15H, aromatic protons). ^{13}C NMR (125 MHz, C_6D_6 , 303 K): δ 11.1 (q, $^1J_{\text{CH}} = 128$ Hz, C_5Me_5), 20.6 (d, $^1J_{\text{CH}} = 139$ Hz, $\beta\text{-C}$), 63.6 (t, $^1J_{\text{CH}} = 139$ Hz, $-\text{CH}_2$), 64.0 (t, $^1J_{\text{CH}} = 140$ Hz, $-\text{CH}_2$), 89.7 (d, $^1J_{\text{CH}} = 134$ Hz, $\alpha\text{-C}$), 92.1 (d, $^1J_{\text{CH}} = 132$ Hz, $\alpha\text{-C}$), 112.3 (d, $^1J_{\text{CH}} = 158$ Hz), 117.2 (s, C_5Me_5), 119.0 (s), 120.1 (d, $^1J_{\text{CH}} = 159$ Hz), 120.2 (d, $^1J_{\text{CH}} = 159$ Hz), 122.4 (d, $^1J_{\text{CH}} = 159$ Hz), 122.5 (d, $^1J_{\text{CH}} = 158$ Hz), 130.5 (s), 131.9 (s), 132.1 (d, $^1J_{\text{CH}} = 159$ Hz), 136.5 (d, $^1J_{\text{CH}} = 161$ Hz), 140.4 (s), 149.1 (s), 151.0 (s), 159.2 (s). The other peaks of aromatic carbons were overlapped by C_6D_6 . Anal. Calcd for $\text{C}_{37}\text{H}_{37}\text{Ta}$: C, 67.07; H, 5.63. Found: C, 66.37; H, 5.69.

Polymerization of Norbornene. In a typical reaction, a solution of **2a** (15 mg, 0.027 mmol) in toluene (1.0 mL) was mixed with a solution of norbornene (100 equiv, 2.7 mmol) in toluene (1.36 M, 2.0 mL) at 25 °C. After the solution was stirred at 45 or 65 °C for a prescribed period (Table 3), methanol (20 mL) was added to the resulting reddish brown solution to precipitate a pale yellow polymer. The polymer was washed with methanol and then dried in vacuo. Bulk polymerizations were run by the reaction of **2a** (15 mg, 0.027 mmol) and norbornene (1000 equiv, 27 mmol) at 65 °C. ^1H NMR (270 MHz, C_6D_6 , 303 K): δ 1.21 (q (br)), 1.49 (br), 1.92 (br), 2.09 (br), 2.95 (br), 5.39 (br), 6.46 (d (br), $^3J_{\text{HH}} = 10.9$ Hz, $=\text{CHPh}$), 7.04–7.33 (m (br), $=\text{CHC}_6\text{H}_5$). $^{13}\text{C}\{^1\text{H}\}$ NMR (68 MHz, C_6D_6 , 303 K): δ 33.6 (C^1), 39.1 (C^2), 43.2 (C^3), 134.2 (C^4).

Comparison of ^1H NMR spectral data with that of the literature^{7,8} determined the stereochemistry of the double bond to be *cis*. Unfortunately, the ^{13}C NMR spectrum of poly(norbornene) displayed no m/r splittings.

GPC Analysis of Poly(norbornene). Gel permeation chromatographic (GPC) analyses were carried out for polymers obtained by using **3** and **6** as catalysts at 40 °C using a Shimadzu LC-10A liquid chromatograph system and a RID-10A differential refractometer, equipped with a Shodex KF-806L column. THF was used as the eluent at a flow rate of 0.8 mL/min, with sample concentrations of 0.5 mg/mL. The GPC column was calibrated with commercially available polystyrene standards (Aldrich).

For polymers obtained by using other complexes as catalysts, GPC analyses were carried out using Tosoh TSKgel HXL-H and L columns connected to a Tosoh UV-8010 absorbance detector. Samples were prepared in THF (0.1–0.3% (w/v)) and were filtered through an Advantec DISMIC-25JP filter in order to remove particulates before injection. GPC columns were calibrated versus commercially available polystyrene standards (Polymer Laboratories Ltd.) whose molecular weight ranged from 500 to 1.11×10^6 .

Hydrogenation of Poly(norbornene). Polymers were hydrogenated with diimine generated in situ from *p*-toluenesulfonylhydrazide.²⁶ Typically, 50 mg samples of polymer were dissolved, with heating, in 10 mL of xylene followed by the addition of 1.5 g of *p*-toluenesulfonylhydrazide. The mixture was stirred at 120 °C for 2.5 h and then poured into methanol. The precipitated polymer was recovered by centrifugation, washed several times with methanol, and dried under vacuum to yield the hydrogenated product in almost quantitative yield. Results of the hydrogenated polymer are shown in Table 4.

Table 6. Crystal Data and Data Collection Parameters of 8

formula	$\text{C}_{18}\text{H}_{23}\text{Cl}_2\text{Ta}$
fw	491.23
cryst syst	monoclinic
space group	$P2_1/a$
<i>a</i> , Å	15.029(3)
<i>b</i> , Å	8.280(3)
<i>c</i> , Å	15.527(3)
β , deg	115.63(1)
<i>Z</i>	4
<i>V</i> , Å ³	1742.1(7)
<i>D</i> _{calcd} , g/cm ⁻³	1.873
<i>F</i> (000)	952
radiation	Mo K α
cryst size, mm	$0.2 \times 0.2 \times 0.2$
abs coeff, cm ⁻¹	65.98
scan mode	$\omega-2\theta$
temp, °C	23
scan speed, deg/min	16
scan width, deg	$0.89 + 0.30 \tan \theta$
$2\theta_{\text{max}}$, deg	55.0
unique data	4286 ($R_{\text{int}} = 0.026$)
unique data ($I > 3\sigma(I)$)	3111
no. of variables	190
<i>R</i>	0.033
<i>R</i> _w	0.035
GOF	2.48
Δ , e Å ⁻³	0.95, -1.17

Table 7. Crystal Data and Data Collection Parameters of 12

formula	$\text{C}_{25}\text{H}_{29}\text{Ta}$
fw	510.45
cryst syst	monoclinic
space group	<i>Cc</i>
<i>a</i> , Å	13.005(3)
<i>b</i> , Å	17.733(5)
<i>c</i> , Å	10.187(3)
β , deg	116.89(2)
<i>Z</i>	4
<i>V</i> , Å ³	2095(1)
<i>D</i> _{calcd} , g/cm ⁻³	1.618
<i>F</i> (000)	1008
radiation	Mo K α
cryst size, mm	$0.3 \times 0.2 \times 0.1$
abs coeff, cm ⁻¹	52.43
scan mode	$\omega-2\theta$
temp, °C	23
scan speed, deg/min	16
scan width, deg	$1.57 + 0.35 \tan \theta$
$2\theta_{\text{max}}$, deg	55.0
unique data	2487 ($R_{\text{int}} = 0.040$)
unique data ($I > 3\sigma(I)$)	2058
no. of variables	251
<i>R</i>	0.024
<i>R</i> _w	0.025
GOF	1.31
Δ , e Å ⁻³	0.59, -0.68

Crystallographic Data Collections and Structure Determination of 8, 12, 14, and 15. Data Collection. The crystals of **8**, **12**, **14**, and **15** suitable for X-ray diffraction studies were sealed in glass capillaries under an argon atmosphere, and then each crystal of the complexes was mounted on a Rigaku AFC-5R four-circle diffractometer for data collection using Mo K α radiation. Relevant crystal and data statistics are summarized in Tables 6–9. The unit cell parameters at 23 °C were determined by a least-squares fit to 2θ values of 20 strong higher reflections for all complexes. Three standard reflections were chosen and monitored every 150 reflections. For each complex, an empirical absorption correction was carried out on the basis of azimuthal scans. No sample showed any significant intensity decay during the data collection. The data for all complexes were corrected for Lorentz and polarization effects.

Table 8. Crystal Data and Data Collection Parameters of 14

formula	C ₂₇ H ₃₁ Nb
fw	448.45
cryst syst	monoclinic
space group	<i>P</i> 2 ₁ / <i>n</i>
<i>a</i> , Å	8.490(5)
<i>b</i> , Å	20.075(5)
<i>c</i> , Å	12.954(4)
β , deg	93.25(3)
<i>Z</i>	4
<i>V</i> , Å ³	2204(1)
<i>D</i> _{calcd} , g/cm ⁻³	1.351
<i>F</i> (000)	936.00
radiation	Mo K α
cryst size, mm	0.3 \times 0.3 \times 0.2
abs coeff, cm ⁻¹	5.55
scan mode	ω -2 θ
temp, °C	23
scan speed, deg/min	16
scan width, deg	1.10 + 0.30 tan θ
2 θ _{max} , deg	55.0
unique data	4295 (<i>R</i> _{int} = 0.048)
unique data (<i>I</i> > 3 σ (<i>I</i>))	1439
no. of variables	254
<i>R</i>	0.079
<i>R</i> _w	0.084
GOF	3.09
Δ , e Å ⁻³	1.08, -0.58

Table 9. Crystal Data and Data Collection Parameters of 15

formula	C ₃₇ H ₃₇ Ta
fw	662.65
cryst system	monoclinic
space group	<i>P</i> 2 ₁ / <i>c</i>
<i>a</i> , Å	13.989(4)
<i>b</i> , Å	10.871(3)
<i>c</i> , Å	18.257(3)
β , deg	94.83(1)
<i>Z</i>	4
<i>V</i> , Å ³	2766.6(10)
<i>D</i> _{calcd} , g/cm ⁻³	1.591
<i>F</i> (000)	1328
radiation	Mo K α
cryst size, mm	0.3 \times 0.2 \times 0.1
abs coeff, cm ⁻¹	39.92
scan mode	ω -2 θ
temp, °C	23
scan speed, deg/min	16
scan width, deg	1.05 + 0.35 tan θ
2 θ _{max} , deg	55.0
unique data	6684 (<i>R</i> _{int} = 0.041)
unique data (<i>I</i> > 3 σ (<i>I</i>))	4397
no. of variables	431
<i>R</i>	0.036
<i>R</i> _w	0.038
GOF	1.55
Δ , e Å ⁻³	1.18, -2.16

Structural Determinations and Refinements. Based on the systematic absence of **8**, (*h*0*l*) with *h* = odd and (0*k*0)

with *k* = odd, the space group of **8** was determined to be *P*2₁/*a*. The systematic absence of (*hkl*) with *h* + *k* = odd and (*h*0*l*) with *l* = odd in the data collected for complex **12** indicated the space group to be *Cc*. Similarly, the systematic absences of **14** and **15** led the space group of **14** and **15** to be *P*2₁/*n* and *P*2₁/*c*, respectively. The structures of all complexes were solved by a direct method (SHELXS 86)⁴⁹ and refined by the full-matrix least-squares method. Measured nonequivalent reflections with *I* > 3.0 σ (*I*) were used for the structure determination. In the subsequent refinement the function $\sum \omega(|F_o| - |F_c|)^2$ was minimized, where $|F_o|$ and $|F_c|$ are the observed and calculated structure factor amplitudes, respectively. The agreement indices are defined as $R = \sum ||F_o| - |F_c|| / \sum |F_o|$ and $R_w = [\sum \omega(|F_o| - |F_c|)^2 / \sum \omega |F_o|^2]^{1/2}$, where $\omega^{-1} = \sigma^2(F_o) = \sigma^2(F_o^2) / (4F_o^2)$. The positions of all non-hydrogen atoms for all complexes were found from a difference Fourier electron density map and refined anisotropically. For **8** and **14** all hydrogen atoms were placed in calculated positions (C–H = 0.95 Å) and kept fixed. For **12**, four hydrogen atoms including H(11) bound to the benzyldiene carbon were found from a difference Fourier map and refined isotropically, and the other hydrogen atoms were placed in calculated positions (C–H = 0.95 Å) and constrained to ride on their respective carbon atoms. Hydrogen atoms of the Cp⁺ ligand of **15** were placed in calculated positions (C–H = 0.95 Å), and the other hydrogen atoms of **15** were found from a difference Fourier syntheses and were refined isotropically. All calculations were performed using the TEXSAN crystallographic software package, and illustrations were drawn with ORTEP.

Acknowledgment. K.M. acknowledges the support by the Grant-in-Aid for Scientific Research on Priority Areas (No. 283, "Innovative Synthetic Reactions") from the Ministry of Education, Science, Sports and Culture, Japan. K.M. also appreciates financial support from the Asahi Glass Foundation.

Supporting Information Available: Tables of final positional parameters, final thermal parameters, bond distances and angles, and best planes for **8**, **12**, **14**, and **15** together with their drawings with an all atom-numbering scheme (58 pages). Ordering information is given on any current masthead page.

OM9802966

(49) Sheldrick, G. M. In *Crystallographic Computing 3*; Sheldrick, G. M., Krüger, C., Goddard, R., Eds.; Oxford University Press: Oxford, 1985; p 179.

(50) Hamilton, J. G.; Ivin, K. J.; Rooney, J. J. *J. Mol. Catal.* **1985**, 28, 255.